Formation of MoS_2 Inorganic Fullerenes (IFs) by the Reaction of MoO_3 Nanobelts and S

Xiao Lin Li and Ya Dong Li*[a]

Abstract: The reaction of MoO_3 and S at temperatures higher than 300 °C in an argon atmosphere provides a convenient and effective method for the synthesis of MoS_2 nanocrystalline substances. MoS_2 nanotubes and fullerene-like nanoparticles have been obtained by the reaction at 850 °C under well-controlled conditions. The influences of reaction temperature and duration were carefully investigated in this paper. All of the nanostructures were characterized by X-ray powder diffraction (XRD), transmission electron microscopy (TEM), and high-resolution transmission electron microscopy (HRTEM). A stepwise reaction model and rolling mechanism were proposed based on the experimental results.

Keywords: fullerenes · inorganic fullerenes · molybdenum · rolling mechanism

Introduction

The discovery of carbon fullerenes and nanotubes, their outstanding properties, and their potential applications has generated intense experimental and theoretical interest.[1–3]. In the search for two-dimensional lamellar structures that are between pure carbon structures and inorganic materials, various layered compounds, such as BN, MoS_2, WS_2, $NiCl_2$, and VO_x, have been found that crystallize in fullerene-like hollow-cage nanostructures and nanotubes under certain experimental conditions.[4–7]. Due to the unique physicochemical properties and numerous potential applications of inorganic fullerenes (IFs), more effort has been devoted to the synthesis of nanoscale one-dimensional structures, especially nanotubes. Up to now, various synthetic strategies have been developed, and many new IFs, including $K_4Nb_6O_{17}$, $MoSe_2$, WSe_2, NbS_2, ReS_2, ZrS_2, and HfS_2 have been obtained.[8–12].

Among these IFs, MoS_2 and WS_2, which were first reported by Tenne et al.,[5] attracted most of the interest for their interesting properties and important applications as solid lubricants, solid-state secondary lithium battery cathodes, and industrial catalysts for hydrodesulfurization of crude oil.[13–15] Recently the excellent performances of MoS_2 nanotubes in hydrogen storage, host–guest compounds, and scanning tunneling microscope (STM) tips have been reported.[16–18] Quite a few methods have been developed for the synthesis of MoS_2 fullerenes. For example, Tenne and co-workers reported the production of MoS_2 IF by the gas-phase reaction between MoO_3 and H_2S in a reducing atmosphere at high temperature.[5, 19] By using a relatively low temperature of about 400 °C for the decomposition of ammonium thiomolybdate within alumina template, Dorhout et al. obtained MoS_2 nanotubes, but with poor crystallinity.[20] Rao et al. employed a high-temperature (~1300 °C) annealing process, and obtained nanotubes of better crystallinity.[21] However developing new synthetic strategies and further understanding of the formation mechanism of MoS_2 nanotubes, fullerene-like nanoparticles are still challenges for scientists. Remskar met the challenge and developed a catalyzed transport method for the self-assembly preparation of single-walled MoS_2 nanotubes.[22] By simply heating MoS_2 powder, Walton et al. developed an alternate route for the synthesis of MoS_2 nanotubes.[23] In this manuscript we first report the synthesis of MoS_2 IF by the reaction of MoO_3 nanobelts and S in an argon atmosphere at high temperature. A possible reaction model and the morphology formation mechanism are proposed on the basis of the experimental facts. Using sulfur as the reactant, instead of the toxic, hazardous, and corrosive H_2S (or mixed gas of H_2S and H_2), our approach is a simple and environmental benign method. This synthetic strategy may offer an opportunity for further investigation on MoS_2, and will serve as a general method for the synthesis of transitional metal dichalcogenides.

[a] Prof. Y. D. Li, X. L. Li
Key Laboratory of Atomic & Molecular Nanosciences
(Ministry of Education, China) Department of Chemistry
Tsinghua University, Beijing, 100084 (P. R. China)
Fax: (+86) 10-62788765
E-mail: ydli@tsinghua.edu.cn

Experimental Section

Materials: Molybdenum trioxide (MoO_3) nanobelts, which were synthesized by us through the solution-phase reaction of sodium molybdate

DOI: 10.1002/chem.200204635

(Na_2MoO_4) and perchloric acid ($HClO_4$), were used as the starting material.[24] All chemicals used in this manuscript were analytical grade reagents.

Synthesis of MoS_2 IF: The preparation of molybdenum disulfide (MoS_2) inorganic fullerenes was carried out in a conventional tube furnace at 850 °C with the argon flow rate of about 20 sccm (standard cubic centimeter per minute). Pre-synthesized 0.4 g molybdenum trioxide (MoO_3) nanobelts and excess sulfur (about 2 g) were loaded in two individual quartz boats and quickly pushed into the hot zone of the furnace, the furnace temperature of which should be stable at about 850 °C. Molybdenum trioxide (MoO_3) nanobelts and sulfur were placed in the middle (~850 °C) and upstream side (~400 °C) of the quartz tube, respectively. After calcination at 850 °C for 2 h, the system was cooled to room temperature under argon, and black molybdenum disulfide (MoS_2) was obtained in the yield of almost 100 %.

Characterization: Powder X-ray diffraction (XRD) was performed on a Bruker D8-Advance X-ray diffractometer with $Cu_{K\alpha}$ radiation ($\lambda =$ 1.54178 Å). The 2θ range used in the measurement was 1.5–70° in steps of 0.02° with a count time of 1 s. The size and morphology of as-synthesized samples were determined by using a Hitachi model H-800 transmission electron microscope (TEM), with a tungsten filament at an accelerating voltage of 200 kV. The structure and composition of the products were characterized by means fo a high-resolution transmission electron microscope (HRTEM, JEOL-2010F) and energy dispersive X-ray spectroscopy (EDS). The surface area of the sample was measured with nitrogen adsorption at −196 °C on a Chemsorb-3000 instrument.

Results and Discussion

Figure 1 shows the XRD pattern of the as-synthesized MoS_2 IF, for which all the reflections have been indexed to the pure hexagonal MoS_2 with lattice constants $a = 3.160$, $c = 12.29$ Å (JCPDS card No: 77–1716). The prominence of the (002) peak indicates the presence of a well-stacked layered

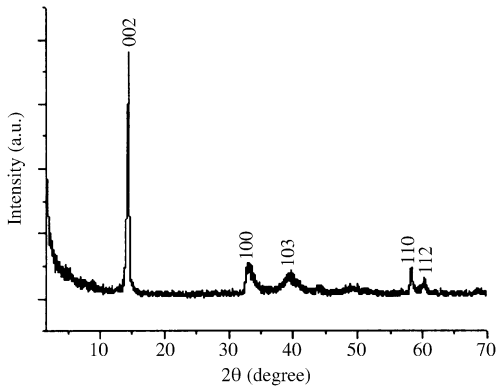

Figure 1. XRD pattern of as-synthesized MoS_2 inorganic fullerenes.

structure. The shift of the (002) peak in the XRD pattern, which is usually regarded as a key mechanism for strain relief of the folded structure,[5, 19] was also observed in our further investigation. The shift of the (002) peak was calculated to be about 0.8 %, which was smaller than that (about 2 %) reported by Tenne et al.[5, 19]

A series of TEM images of MoS_2 nanotubes are shown in Figure 2a–f. On the basis of TEM measurements, most of the nanotubes obtained by our method have sealed ends and the diameters change from one tube to the next. In Figure 2a–c representative MoS_2 nanotubes with the diameters of about 30, 150, and 330 nm, respectively, are shown. Further observation showed that the MoS_2 nanotube depicted in Figure 2a had a collapsed end; this might indicate some relationship between nanotubes and nanorods. HRTEM patterns (Figure 2d–f) provide further insight into the structure of individual MoS_2 nanotubes. In all HRTEM images, the distance between the two lattice fringes is 0.62 nm. The selected area electron diffraction (SAED) pattern taken on an individual nanotube is shown in the inset of Figure 2f. The prolonged diffraction points of the ED pattern indicated the orientation.

Figure 3a,b depict typical TEM images of fullerene-like MoS_2 nanoparticles. As shown in the images, these particles synthesized by our method usually have a large diameter and elongated shape, and can be regarded as short nanotubes with both ends closed. Defects could be found in the wall of those hollow-cage nanostructures.

The energy dispersive X-ray spectra (EDS) have been recorded for individual MoS_2 nanotubes and fullerene-like nanoparticles; they confirmed that sulfur and molybdenum atoms were in the molar ratio of about 2:1 (spectra were not shown).

MoS_2 samples were dehydrated with a flow of dry nitrogen at 180 °C for 5 h before the adsorption measurement. The surface area, determined by the Brunauer–Emmet–Teller (BET) gas adsorption isothermals, was found to be about 50 $m^2 g^{-1}$. With this large surface area, as-synthesized MoS_2 IFs are expected to have excellent performance in catalysis, catalysts carriers, and hydrogen storage, etc.

Influences of the reaction temperature and duration: A series of experiments have been conducted for a better understanding of the reaction between MoO_3 nanobelts and sulfur.

The influence of temperature was investigated from 200–900 °C. The results showed that MoS_2 IFs could only be obtained at about 850 °C, although the reaction of MoO_3 and S happened at a rather low temperature. Figure 4 shows typical XRD patterns of the samples obtained at 300 °C, 400 °C, 500 °C, and 900 °C. As can be seen, the reaction was not complete even after two hours reaction at 300 °C, and MoS_2 and MoO_3 were found to coexist. However, when the temperature was higher than 400 °C, pure hexagonal MoS_2 was the only product. TEM images of the corresponding samples obtained at 400 °C, 500 °C, and 900 °C are shown in Figure 5a–c, respectively, in which MoS_2 folded layers (Figure 5a and b) and large blocks (Figure 5c) are observed.

To investigate the detail of the reaction processes of MoO_3 with S, we took samples at different reactions times. The corresponding samples were examined by XRD, and typical results at 500 °C and 850 °C are provided in Figure 6. Figure 6a shows the XRD patterns of samples measured A) after 30 min, 500 °C and B) after 2 h, 500 °C. Figure 6b shows the XRD patterns of samples measured A) after 10 min, 850 °C; B) after 30 min, 850 °C; and C) after 2 h, 850 °C. In addition to the fact that a signal due to MoO_3 was observed in the reaction product of the sample taken after a short time at the lower temperature (Figure 6a (A)), an important fact was found that no matter at what temperature the reaction was carried out, a short reaction time leads to the coexistence of MoO_2 and MoS_2. It was believed that MoO_2 is an intermediate product.

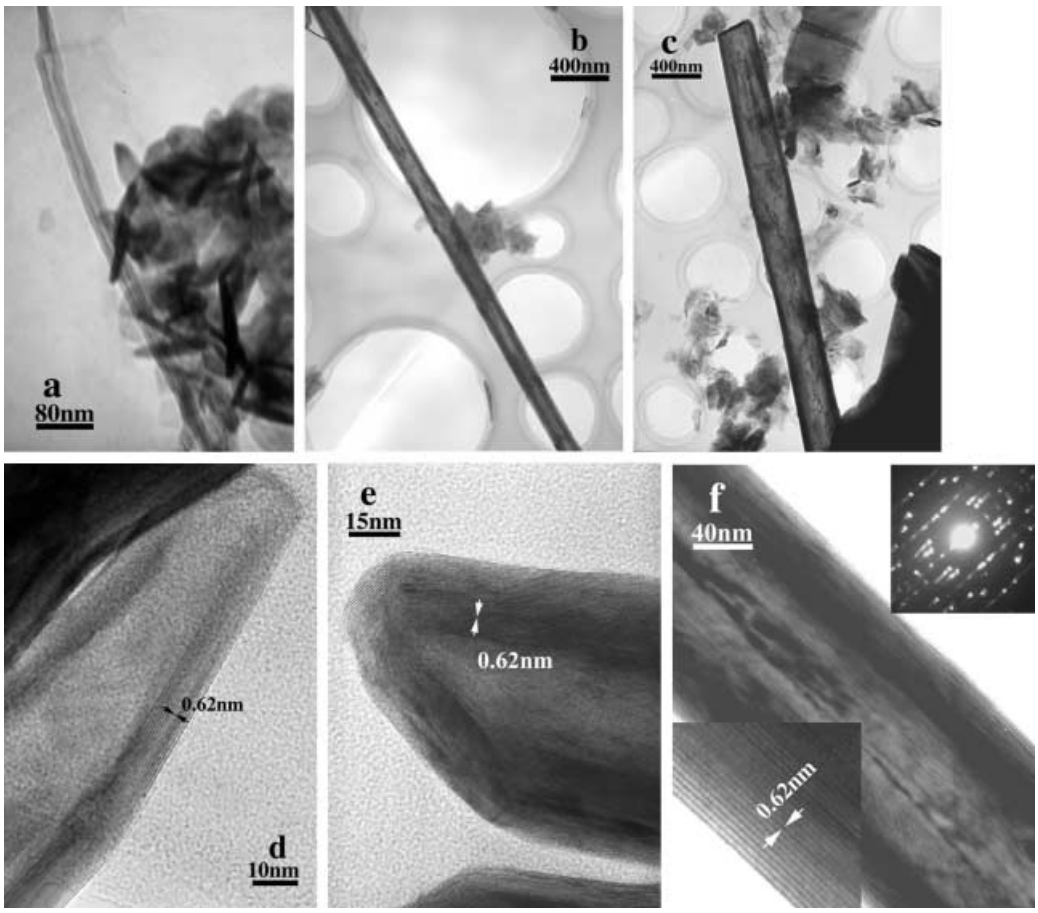

Figure 2. Representative TEM images of MoS_2 nanotubes with different diameters: a–c) low-magnification TEM images and d–f) HRTEM images of MoS_2 nanotubes. a) Nanotube with diameter of about 30 nm. b) Nanotube with diameter of about 150 nm. c) Nanotube with diameter of about 330 nm. The distance between two fringes is 0.62 nm. The insets in f) are of an enlarged pattern of the tube wall and a SAED pattern taken on the individual nanotube.

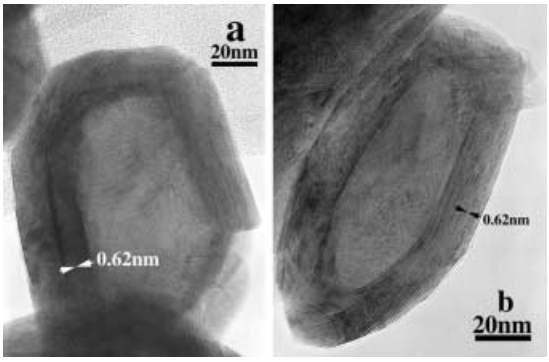

Figure 3. HRTEM images of as-synthesized fullerene-like MoS_2 nanoparticles. The distance between the lattice fringes is 0.62 nm.

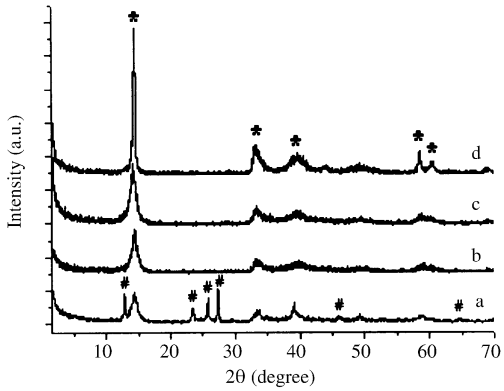

Figure 4. XRD patterns of the final products obtained at different temperatures: a) 300 °C, b) 400 °C, c) 500 °C, and d) 900 °C. (*: MoS_2 peaks, #: MoO_3 peaks).

Reaction mechanism: Reported strategies in the synthesis of MoS_2, especially the gas-phase reaction of MoO_3 with H_2S in the reducing atmosphere of H_2, give us much inspiration towards understanding the reaction mechanism of MoO_3 with S.[5, 19, 25] Niemantsverdriet et al. investigated the basic reaction steps in the sulfurization of MoO_3 by in situ spectra detection, and provided strong evidence for the existence of intermediate products, such as MoO_2 and $MoOS_2$.[26] Tenne et al. have studied the kinetic process of the reaction of MoO_3 with H_2S, and proposed a synergetic substitution–reduction model for the reaction process.[5, 19] It was believed that MoS_2 formed as the result of the stepwise reaction of substitution and reduction, which happened first at the terminal oxygen ($Mo=O_t$) of MoO_3.[5, 19, 26]

The well-known reaction of MoO_3 with H_2S in an H_2 atmosphere are given in Equations (1) and (2).[5, 19]:

$$MoO_3 + xH_2 \rightarrow MoO_{3-x} + xH_2O \quad (1)$$

$$MoO_{3-x} + (1-x)H_2 + 2H_2S \rightarrow MoS_2 + (3-x)H_2O \quad (2)$$

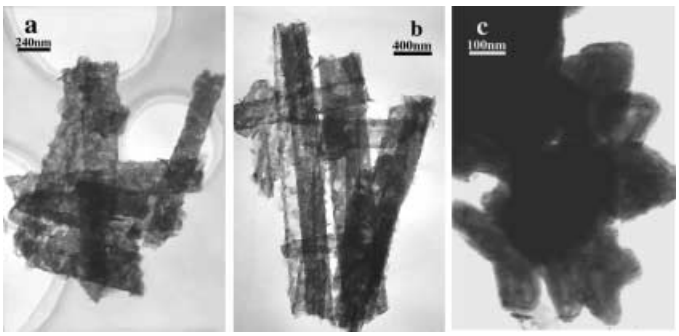

Figure 5. TEM images showing the typical morphology of MoS_2 samples obtained at different temperatures: a) 400 °C, b) 500 °C, and c) 900 °C.

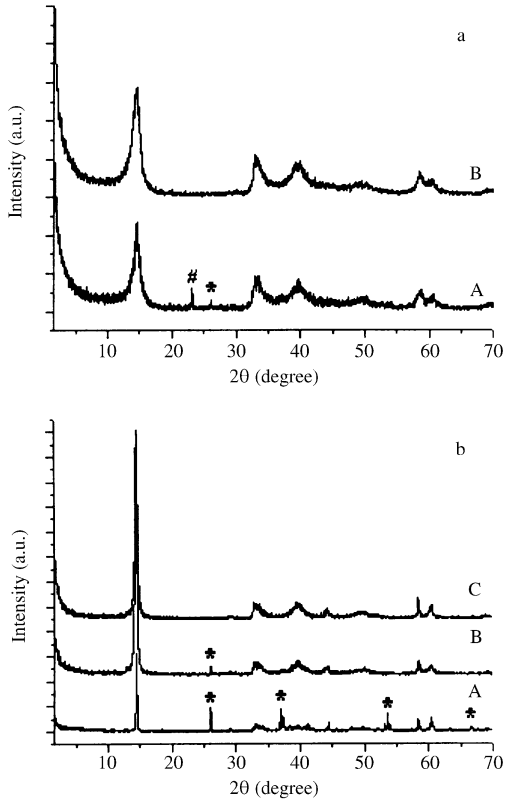

Figure 6. XRD patterns obtained for different reaction duration at the temperatures of 500 °C and 850 °C: a) 500 °C; A) 30 min, B) 2 h; b) 850 °C; A) 10 min, B) 30 min, C) 2 h. (*: signal of MoO_2, #: signal of MoO_3.)

In our strategy, sulfur instead of H_2S and H_2 served as the reductant and sulfurization agent at the same time. The reaction between MoO_3 and S is given in Equation (3).

$$2MoO_3 + 7S \rightarrow 2MoS_2 + 3SO_2 \quad (3)$$

Although the exact reaction processes of MoO_3 with S has not been completely resolved at this stage, analogy can be drawn between the reaction of MoO_3 with H_2S and our method. We too found MoO_2 as the intermediate product in our method (Figure 6). Taking reports in the literature[5, 19, 26] into account together with our experiment results, we postulate that the reaction model for MoO_3 and S might also involve the stepwise reduction and sulfurization. A possible stepwise reaction process of MoO_3 and S is given in Equations (4) and (5).

$$MoO_3 + x/2\,S \rightarrow MoO_{3-x} + x/2\,SO_2 \quad (4)$$

$$MoO_{3-x} + (7-x)/2\,S \rightarrow MoS_2 + (3-x)/2\,SO_2 \quad (5)$$

When the reaction duration is short, the sulfurization process is not complete and intermediate products can be obtained. MoO_2, as one of the most stable oxides of molybdenum, is the most common intermediate product (Figure 6).

By substituting $x = 1$ in Equation (4), MoO_2 becemes the reaction product [Eq. (6)].

$$MoO_3 + \tfrac{1}{2}S \rightarrow MoO_2 + \tfrac{1}{2}SO_2 \quad (6)$$

An immediate application for this kind of reaction has been found. By using MoO_3 nanobelts and Se as the reactants, we have obtained $MoSe_2$. WS_2 was also obtained by the reaction of WO_3 and S. Synthesis of other transition metal dichalcogenides are still under investigation.

Mechanism for the formation of MoS_2 IF: Many techniques have been developed for the synthesis of inorganic fullerenes,[5–12, 19–23, 27] and a number of studies have been focused on the formation mechanism of those novel nanostructures. On account of the bending of graphite sheets under high temperature or electron beam irradiation[28] and rolling phenomena in the synthesis of many nanotubes,[29–36] curling of the moleculars layers followed by adhesion was proposed to be responsible for the tube-formation process. In the synthesis of Bi and WS_2 nanotubes and W nanowires, we have found that one-dimensional nanostructures can be obtained through the rolling of either a natural or an artificial lamellar structure.[30–32] Remskar and co-workers obtained direct evidence for the derivation of tubules from the bending of platelets.[33] Mallouk and Domen also provided clear evidence of chemical transformation of lamellar oxides into tubular structures, and interpreted the layering of structures as a rolling process.[8, 34] We postulate that the formation mechanism of MoS_2 nanotubes and fullerene-like nanoparticles synthesized by our approach might also involve rolling from its quasi-layered structure.

TEM images shown in Figure 7a–e provide evidence of the fact that MoS_2 nanotubes are formed by the rolling process. Figure 7a shows the HRTEM image of a nanotube with a closed end. The defective structure of the closed end is an indication that it was formed by the bending or rolling of the tube wall. This observation provides clues for the rolling mechanism in explaining the formation of nanotubes that have closed ends. Some inner broken layers were noticed in the nanotube shown in Figure 7b. The formation of those broken layers was ascribed to the interruption during the rolling process to form a closed-end tube. Samples at different stages of rolling are observed in the regions marked A, B, and C in Figure 7c. Following the rolling sequence of A → B → C, nanotubes and nanorods are believed to form. Moreover, although we believe that a sheet might begin to roll at both

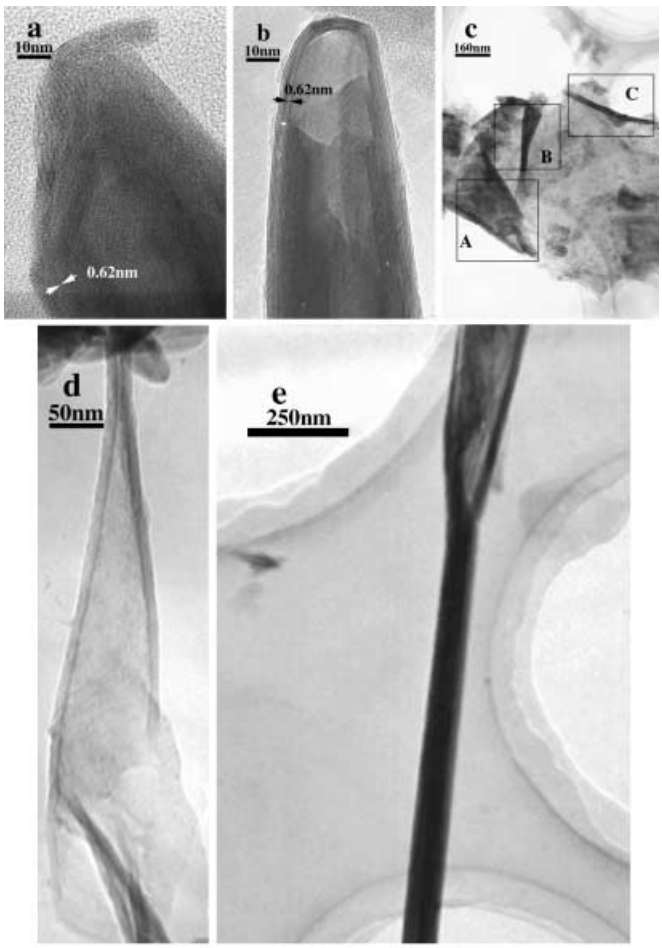

Figure 7. TEM images showing the evidence of rolling process in the formation of fullerene-like MoS_2 nanoparticles, nanotubes and nanorods. a) Nanotube with closed end, formed by rolling. b) Nanotube with some inner layers broken during the rolling process to form a closed end. c) MoS_2 layers at different rolling stages A → B → C showing the transition from a plate-like structure to a tubular structure. d) Half-tube and half-plate nanostructure. e) Half-rod and half-plate nanostructure.

edges, this was the first time that we observed this phenomenon. More direct evidence for the rolling mechanism is found in the half-tube/half-rod and half-plate structure, as shown in Figure 7d–e. Figure 7d shows the coexistence of both nanotubes and rolling sheets in the same structure. The half-rod and rolling sheet structure shown in Figure 7e indicates that one-dimensional nanorods might be formed by the rolling mechanism. Fullerene-like MoS_2 nanoparticles obtained by our method usually have an elongated shape and a large diameter, and can be regarded as short nanotubes with both ends closed. Analogously to the nanotube shown in Figure 7a, the defective wall of fullerene-like MoS_2 nanoparticles (Figure 3) indicates that they were formed by the rolling of MoS_2 layers. With a rather large diameter, as-synthesized fullerene-like nanoparticles, as well as the nanotubes, could not be formed by other processes such as surface sulfurization of MoO_3, because it is hard to imagine that the inner core could be consumed completely, leaving a just thin shell.

Recently Yada et al. reported the formation of tubular structures through the folding of flexible aluminium-based layers.[35] SiGe nanotubes have also been synthesized by rolling from a thin layer of SiGe.[36] It is foreseeable that the rolling mechanism may become a general method for the growth of IF and nanorods.

In contrast to the analogous IFs of WS_2, which can be formed from solid WO_3 nanoparticles, so far the formation of MoS_2 IFs from pre-prepared MoO_3 was not possible, for the simple reason that MoO_3 nanoparticles are very volatile above 650 °C. Therefore, although synthesis of fullerene-like MoS_2 nanoparticles has been achieved by evaporation–condensation and sulfurization of MoO_3,[19] MoS_2 nanotubes are not easily synthesized. In our strategy, however, we overcame the volatilization of MoO_3 and obtained MoS_2 IF by placing MoO_3 nanobelts and S into the hot zone of the furnace after the furnace temperature had stabilized at about 850 °C. At 850 °C the reaction of MoO_3 and S was very fast and MoO_3 sublimation was not instantaneous. So the immediate formation of MoS_2 thin layers restrains the sublimation of MoO_3 nanobelts. In addition, the formation of MoO_{3-x} or MoO_2 cores decreased the volatilization of the MoO_3 nanobelts. Hence, in our synthesis, MoO_3 nanobelts were not volatile. MoO_3 and S reacted on the surface of the nanobelts, and immediately formed an MoS_2 thin film, which is indispensable in the rolling mechanism. Under appropriate controlled conditions, including the flow speed of argon, the interaction between neighboring layers could be reduced at the edges of the layer, while keeping the interactions of in-layer atoms or molecules; thus a newly formed MoS_2 thin film can wrap up and folded back on itself to form a tubular structure. The rolling process may begin at one or both edges of the MoS_2 layers. If the scroll-like tubular structure is maintained throughout the reaction, MoS_2 nanotubes with open ends are obtained. Further bending, rolling, collapse, and restacking at the ends of the tubular structures may cause the formation of IFs with closed ends.

It was worth noting that in agreement with previous reports in the literature[19] the initial size and morphology of the precursor influences the formation of nanotubes. In control experiments with commercial MoO_3 as the starting material, MoS_2 nanoparticles were obtained instead of nanotubes (Figure 8).

Conclusion

In summary, we have developed a new method for the synthesis of MoS_2 nanocrystals and obtained MoS_2 IFs under well-controlled conditions by the reaction of MoO_3 with S. A stepwise reaction model was proposed on the basis of the previous reports and our experimental results. The rolling mechanism was further developed and applied in the formation of MoS_2 nanotubes and fullerene-like nanoparticles. This strategy provides a low cost, large-scale method for the synthesis of MoS_2, and may become a general method for the synthesis of transition metal dichalcogenides.

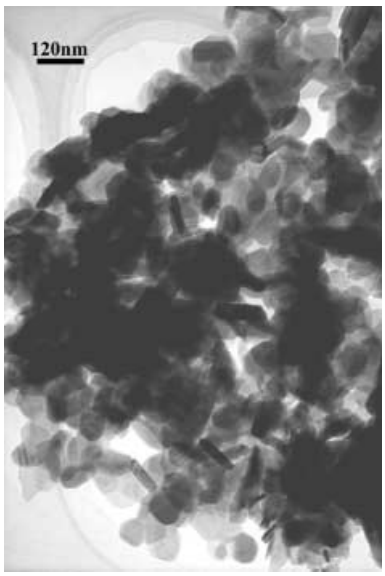

Figure 8. TEM image showing the MoS_2 nanoparticles obtained in control experiments with commercial MoO_3 as the starting material.

Acknowledgement

This work was supported by NSFC (20025102, 50028201, 20151001), the Foundation for the Author of National Excellent Doctoral Dissertation of P. R. China, and the state key project of fundamental research for nanomaterials and nanostructures.

[1] H. W. Kroto, J. R. Heath, S. C. O'Brien, R. F. Crul, R. E. Smalley, *Nature* **1985**, *318*, 162–163.
[2] S. Iijima, *Nature* **1991**, *354*, 56–58.
[3] a) M. S. Dresselhaus, G. Dresselhaus, P. C. Eklund, *Science of Fullerenes and Carbon Nanotubes*, Academic Press, San Diego, **1996**; b) *Carbon Nanotubes-Synthesis, Structure, Properties, and Applications* (Eds.: M. S. Dresselhaus, G. Dresselhause, P. Avouris), Springer, Berlin, **2001**.
[4] N. G. Chopra, R. J. Luyren, K. Cherry, V. H. Crespi, M. L. Cohen, S. G. Louis, A. Zettl, *Science* **1995**, *269*, 966–967.
[5] a) R. Tenne, L. Margulis, M. Genut, G. Hodes, *Nature* **1992**, *360*, 444–446; b) L. Margulis, G. Salitra, R. Tenne, M. Talianker, *Nature* **1993**, *365*, 113–114; c) Y. Feldman, E. Wasserman, D. J. Srolovitz, R. Tenne, *Science* **1995**, *267*, 222–225.
[6] Y. R. Hachohen, E. Grunbaum, J. Sloan, J. L. Hutchison, R. Tenne, *Nature* **1998**, *395*, 336–337.
[7] a) M. E. Spahr, P. Betterli, R. Nesper, M. Miiller, F. Krumeich, H. U. Nissen, *Angew. Chem.* **1998**, *110*, 1339–1342; *Angew. Chem. Int. Ed.* **1998**, *37*, 1263–1265; b) F. Krumeich, H. J. Muhr, M. Niederberger, F. Bieri, B. Schnyder, R. Nesper, *J. Am. Chem. Soc.* **1999**, *121*, 8324–8331; c) M. Niederberger, H. J. Muhr, F. Krumeich, F. Bieri, D. Gunther, R. Nesper, *Chem. Mater.* **2000**, *12*, 1995–2000.
[8] a) G. B. Saupe, C. C. Waraksa, H. N. Kin, Y. J. Han, D. M. Kaschak, D. M. Skinner, T. E. Mallouk, *Chem. Mater.* **2000**, *12*, 1556–1562; b) R. E. Schaak, T. E. Mallouk, *Chem. Mater.* **2000**, *12*, 3427–3434.
[9] M. Nath, C. N. R. Rao, *Chem. Commun.* **2001**, 2236–2237.
[10] a) M. Nath, C. N. R. Rao, *J. Am. Chem. Soc.* **2001**, *123*, 4841–4842; b) C. Schuffenhauer, R. Popovitz-Biro, R. Tenne, *J. Mater. Chem.* **2002**, *12*, 1587–1591; c) Y. Q. Zhu, W. K. Hsu, H. W. Kroto, D. R. M. Walton, *Chem. Commun.* **2001**, 2184–2185.
[11] a) M. Brorson, T. W. Hansen, and C. J. H. Jacobsen, *J. Am. Chem. Soc.* **2002**, *124*, 11582–11583; b) K. S. Coleman, J. Sloan, N. A. Hanson, G. Brown, G. P. Clancy, M. Terrones, H. Terrones, M. L. H. Green, *J. Am. Chem. Soc.* **2002**, *124*, 11580–11581.
[12] M. Nath, C. N. R. Rao, *Angew. Chem.* **2002**, *114*, 3601–3604; *Angew. Chem. Int. Ed.* **2002**, *41*, 3451–3454.
[13] a) M. Chhowalla, G. A. J. Amaratunga, *Nature* **2000**, *407*, 164–167; b) L. Rapoport, Y. Bilik, Y. Feldman, M. Homyonfer, S. R. Cohen, R. Tenne, *Nature* **1997**, *387*, 791–793.
[14] N. Imanishi, K. Kanamura, Z. Takehara, *J. Electrochem. Soc.* **1992**, *139*, 2082–2087.
[15] J. Chen, S. L. Li, Q. Xu, K. Tanaka, *Chem. Commun.* **2002**, 1722–1723.
[16] J. Chen, N. Kuriyama, H. Yuan, H. T. Takeshita, T. Sakai, *J. Am. Chem. Soc.* **2001**, *123*, 11813–11814.
[17] a) A. Zak, Y. Feldman, V. Lyakhovitskaya, G. Leitus, R. Popovitz-Biro, E. Wachtel, H. Cohen, S. Reich, R. Tenne, *J. Am. Chem. Soc.* **2002**, *124*, 4747–4758; b) M. Remskar, Z. Skraba, P. Stadelmann, F. Levy, *Adv. Mater.* **2000**, *12*, 814–818; c) M. Homyonfer, B. Alperson, Y. Rosenberg, L. Sapir, S. R. Cohen, G. Hodes, R. Tenne, *J. Am. Chem. Soc.* **1997**, *119*, 2693–2698.
[18] A. Rothschild, S. R. Cohen, R. Tenne, *Appl. Phys. Lett.* **1999**, *75*, 4025–4027.
[19] a) Y. Feldman, G. L. Frey, M. Homyonfer, V. Lyakhovitskaya, L. Margulis, H. Cohen, G. Hodes, J. L. Hutchison, R. Tenne, *J. Am. Chem. Soc.* **1996**, *118*, 5362–5367; b) R. Tenne, M. Homyonfer, Y. Feldman, *Chem. Mater.* **1998**, *10*, 3225–3238; c) A. Zak, Y. Feldman, V. Alperovich, R. Rosentsveig, R. Tenne, *J. Am. Chem. Soc.* **2000**, *122*, 11108–11116.
[20] C. M. Zelenski, P. K. Dorhout, *J. Am. Chem. Soc.* **1998**, *120*, 734–742.
[21] M. Nath, A. Govindaraj, C. N. R. Rao, *Adv. Mater.* **2001**, *13*, 283–286.
[22] M. Remskar, A. Mrzel, Z. Skraba, A. Jesih, M. Ceh, J. Demsar, P. Stadelmann, F. Levy, D. Milhailovic, *Science* **2001**, *292*, 479–481.
[23] W. K. Hsu, B. H. Chang, Y. Q. Zhu, W. Q. Han, H. Terrones, M. Terrones, N. Grobert, A. K. Cheetham, H. W. Kroto, D. R. M. Walton, *J. Am. Chem. Soc.* **2000**, *122*, 10155–10158.
[24] X. L. Li, J. F. Liu, Y. D. Li, *Appl. Phys. Lett.* **2002**, *81*, 4832–4834.
[25] J. H. Zhan, Z. D. Zhang, X. F. Qian, C. Wang, Y. Xie, Y. T. Qian, *J. Solid State Chem.* **1998**, *141*, 270–273.
[26] T. Weber, J. C. Muijsers, J. H. M. C. van Wolput, C. P. J. Verhagen, J. W. Niemantsverdriet, *J. Phys. Chem.* **1996**, *100*, 14144–14150.
[27] a) R. L. D. Whitby, W. K. Hsu, P. K. Fearon, N. C. Billingham, I. Maurin, H. W. Kroto, D. R. M. Walton, C. B. Boothroyd, S. Firth, R. J. H. Clark, D. Collison, *Chem. Mater.* **2002**, *14*, 2209–2217; b) Y. Q. Zhu, W. K. Hsu, N. Grobert, B. H. Chang, M. Terrones, H. Terrones, H. W. Kroto, D. R. M. Walton, *Chem. Mater.* **2000**, *12*, 1190–1194.
[28] a) R. D. Heidenreich, W. M. Hess, L. L. Ban, *J. Appl. Crystallogr.* **1968**, *1*, 1; b) D. Ugarte, *Nature* **1992**, *359*, 707–709.
[29] R. Bacon, *J. Appl. Phys.* **1960**, *31*, 283–290.
[30] Y. D. Li, J. W. Wang, Z. X. Deng, Y. Y. Wu, X. M. Sun, D. P. Yu, P. D. Yang, *J. Am. Chem. Soc.* **2001**, *123*, 9904–9905.
[31] Y. D. Li, X. L. Li, R. R. He, J. Zhu, Z. X. Deng, *J. Am. Chem. Soc.* **2002**, *124*, 1411–1416.
[32] Y. D. Li, X. L. Li, Z. -X. Deng, B. C. Zhou, S. S. Fan, J. W. Wang, X. M. Sun, *Angew. Chem.* **2002**, *114*, 343–345; *Angew. Chem. Int. Ed.* **2002**, *41*, 333–335.
[33] a) M. Remskar, Z. Skraba, F. Cleton, R. Sanjines, F. Levy, *Appl. Phys. Lett.* **1996**, *69*, 351–353; b) M. Remskar, Z. Skraba, M. Regula, C. Ballif, R. Sanjines, F. Levy, *Adv. Mater.* **1998**, *10*, 246–249; c) M. Remskar, Z. Skraba, R. Sanjines, F. Levy, *Appl. Phys. Lett.* **1999**, *74*, 3633–3635.
[34] a) R. Abe, K. Shinohara, A. Tanaka, M. Hara, J. Kondo, K. Domen, *J. Mater. Res.* **1998**, *13*, 861–865; b) R. Abe, K. Shinohara, A. Tanaka, M. Hara, J. Kondo, K. Domen, *Chem. Mater.* **1997**, *9*, 2179–2184.
[35] M. Yada, H. Hiyoshi, K. Ohe, M. Machida, T. Kijima, *Inorg. Chem.* **1997**, *36*, 5565–5569.
[36] O. G. Schmidt, K. Eberl, *Nature* **2001**, *410*, 168.

Received: December 4, 2002 [F4635]

